Solar Spectrum

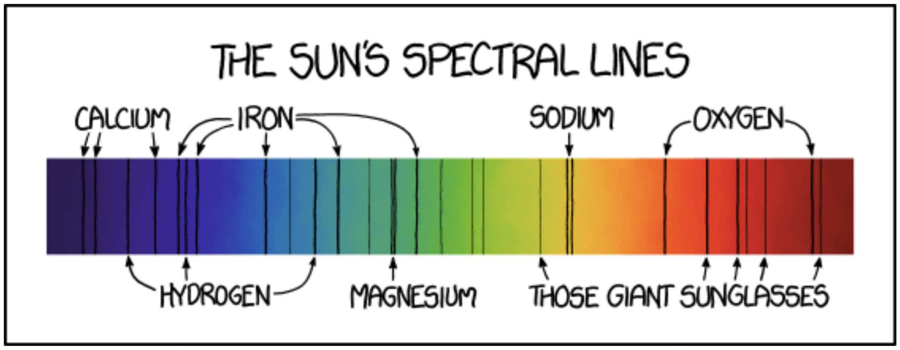

Title text: I still don't understand why the Sun paid the extra money for Transitions lenses.

Figure 1.1. Solar spectrum with interpretation by xkcd comic artist Randall Munroe. [42]

1.2 Abstract

Inverse spectral problems.

Please include a short description of your article including the assumed background of the reader. As a reminder, we are aiming this volume at junior and senior undergraduate math majors. Authors can assume readers have had an introductory course in most standard topics. If your assumptions are different, or more specific, please notate that here.

For the following sections, feel free to change the section titles if needed, to better fit your article and your field of research. Additionally please go ahead and add subsections as needed. If a section below does not make sense for your work go ahead and delete as needed. This is meant to be a general guideline not set in stone.

1.3 Spectral geometry

1.3.1 Can you hear the shape of a drum?

The story of the origin of spectral geometry is beautifully told by Carolyn Gordon and David Webb in the Chauvenet Prize[1] winning article [18]. The background provided below follows the beginning of [18], while going into less detail.

In the 19th century astronomers discovered that they could use the spectrum of light emitted by a star to determine the chemical elements present in the star. This is because each gas in a star, such as hydrogen or helium, absorbs a discrete set of light frequencies that form a distinctive signature of that gas. The xkcd comic in Figure 1.1 shows the spectrum of visible light present in light from the sun. The dark bands in this spectrum, called Fraunhofer lines, indicate missing light frequencies. Missing frequencies match up to the signature light frequencies of gases present in the sun. In fact Helium is named after the Greek sun god Helios because the signature color spectrum of Helium was first detected on the sun [24].

Inspired by this work, in 1882 British physicist Sir Arthur Schuster offered the following observation [18]:

> We know a great deal more about the forces which produce the vibrations of sound than about those which produce the vibrations of light. ... but it would baffle the most skillful mathematician to solve the inverse problem and to find out the shape of a bell by means of the sounds which it is capable of sending out.

The question of determining the shape of a object given only the object's intrinsic harmonic properties has blossomed into a rich field of mathematical study known as inverse spectral geometry. The infinite list of fundamental vibrational frequencies of an object is known to mathematicians as the *Laplace spectrum* of the object.

A first inverse spectral geometry question to consider is "Can we hear the length of a string?" View the the straight line labeled (a) in Figure 1.2 as a string on a harp. When plucked, the string can vibrate in a variety of ways including the standing waves illustrated (b), (c) and (d). The frequency of waveform (b) is the lowest one at which the string can vibrate and corresponds to the pitch of the string. Waveforms (c) and (d) vibrate at increasingly higher frequencies

[1] This prize is awarded by the Mathematical Association of America to recognize the year's top expository writing in mathematics.

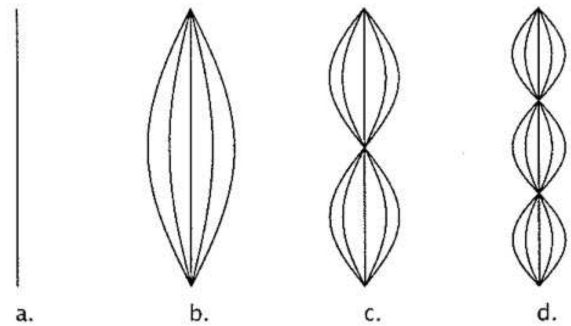

Figure 1.2. Three fundamental oscillations of a string

called first and second overtones of the string, respectively. Dividing the string into bumpier and bumpier oscillations yields an infinite list of standing waves which vibrate at higher and higher frequencies.

These frequencies can be computed by modeling the vibrating string using methods from introductory partial differential equations. First assume the string is stretched out along the x-axis in the Cartesian plane from $x = 0$ to $x = L$. Note we are taking L to be the length of the string. We seek a function $u(t, x)$ that gives the vertical displacement of the string over point x, for $0 \leq x \leq L$, at time t, for $t \geq 0$. To model vibration we require $u(t, x)$ to satisfy the wave equation

$$c^2 \frac{\partial^2 u}{\partial x^2} = \frac{\partial^2 u}{\partial t^2}.$$

The fact that the ends of the string don't move is captured by the requirement for all t. For simplicity we will take constant $c = 1$.

Applying the method of separation of variables[2], we look for solutions u of the form $u(t, x) = A(t)\psi(x)$. This reduces the problem to solving a pair of ordinary differential equations

$$\frac{d^2 A}{dt^2} = -\lambda A \qquad \text{(time differential equation)} \tag{1.1}$$

$$\frac{d^2 \psi}{dx^2} = -\lambda \psi \qquad \text{(space differential equation)} \tag{1.2}$$

for some non-negative constant λ.

But wait, something very exciting has just occurred! Before we use this reduced problem to compute the fundamental vibrational frequencies of our string, lets take a closer look at the space differential equation above. Observe that the process of computing the second derivative of a function is a linear transformation. In fact it is a famous linear transformation: the second derivative operator $\frac{d^2}{dx^2}$ is the 1-dimensional Laplace operator on our interval $[0, L]$. It is the cousin of the 3-dimensional Laplace operator $\frac{\partial^2}{\partial x^2} + \frac{\partial^2}{\partial y^2} + \frac{\partial^2}{\partial z^2}$ that appears in multivariable calculus courses, for example. Let the symbol Δ to denote the Laplace operator in any context. Now observe that the space differential equation asks us to find functions ψ for which the image of ψ under the Laplace operator is simply a scaled copy of ψ back again. We have happened upon the eigenvalue problem $\Delta\psi = \lambda\psi$. This is very exciting because this type of eigenvalue problem is at the core of all of inverse spectral geometry.

Now lets get back to the task at hand. Methods from a first course in differential equations can be used to show that solutions to the time and space differential equations will have the forms

$$A(t) = a\cos(\sqrt{\lambda}t) + b\sin(\sqrt{\lambda}t)$$
$$\psi(x) = c\cos(\sqrt{\lambda}x) + d\sin(\sqrt{\lambda}x)$$

respectively, where a, b, c and d are arbitrary real constants. Applying the condition that $u(t, 0) = u(t, L) = 0$ to solutions to the space differential equation forces c to be zero and $\sqrt{\lambda}L = n\pi$ for n a non-negative integer.

[2]To see this process in full detail see Chapter 10 in [5], for example.

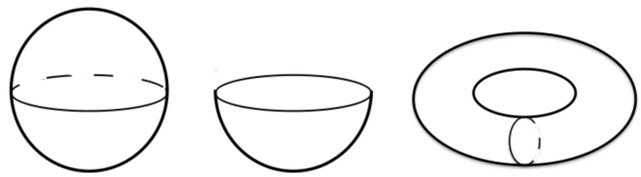

Figure 1.3. Sphere, hemisphere and torus

Assembling these facts back into separated form $u(t,x) = A(t)\psi(x)$ yields a family of solution functions

$$u(t,x) = \left(a\cos\left(\frac{n\pi}{L}t\right) + b\sin\left(\frac{n\pi}{L}t\right)\right)\sin\left(\frac{n\pi}{L}x\right).$$

For a fixed value of t we see that solutions are a scaled sine wave of period $\frac{2L}{n}$ that is zero at the endpoints of the string. Note that n counts the number of 'bumps' in the wave as in Figure 1.2 where wave (b) has one bump, (c) has two bumps, and (d) has three bumps. Letting t vary scales the amplitude of the sine wave, resulting in a standing wave solution to the wave equation that oscillates with frequency $\frac{n}{2L}$.

We can now answer the question of whether or not we can hear the length of a string. The list of fundamental vibrational frequencies (also called harmonics) of the string is $\frac{1}{2L}, \frac{2}{2L}, \frac{3}{2L}, \ldots, \frac{n}{2L}, \ldots$. If we take the reciprocal of the lowest frequency on this list (the pitch of the string) and divide the result by two we recover the length L. So yes, we can hear the length of a string.

Much of the work in inverse spectral geometry examines the properties of objects called Riemannian manifolds. The interval $[0, L]$ in the real line provides a simple example. More generally a Riemannian manifold is a metric space to which the tools of calculus apply. Figure 1.3 illustrates three Riemannian manifolds, from left to right: the sphere, the hemisphere, and the torus. Each object is two-dimensional because we consider only the surface of the object, not its inside. For example the torus is not solid like a donut, instead is like an inner tube where the thickness of the tube's rubber skin is infinitely thin. Each of the surfaces in Figure 1.3 bend smoothly, they have no sharp corners. A sharp corner is a place where the tools of calculus break down and so sharp corners are not allowed on a manifold. First described by Riemann in 1854, Riemannian manifolds have proven to be extremely useful objects. They provide the mathematical language needed to express Einstein's theory of general relativity and now appear frequently in many areas of mathematical physics. Manifolds also possess a expansive mathematical theory apart from their applications.

As with the string, a general Riemannian manifold has an infinite list of fundamental vibrational frequencies. (Here I am assuming the manifold is compact.) So we can ask "can you hear the shape of a manifold?" To make this question mathematically precise we need to return to the vibrating string for a moment. Recall that the space differential equation in line (1.2) can be viewed as the eigenvalue problem $\Delta\psi = \lambda\psi$ where Δ is the 1-dimensional Laplace operator on the interval. The fact that the string has infinite list of harmonics $\frac{1}{2L}, \frac{2}{2L}, \frac{3}{2L}, \ldots, \frac{n}{2L}, \ldots$ is equivalent to the fact that there is an infinite list of eigenvalues λ_n that satisfy the eigenvalue problem $\Delta\psi = \lambda\psi$. The connection is that the nth vibrational frequency is equal to $\frac{\sqrt{\lambda_n}}{2\pi}$. Using the tools of Riemannian geometry, one can define a Laplace operator on any Riemannian manifold that generalizes the familiar Laplace operator on R^n. It can be shown that the eigenvalues of the Laplace operator on a compact Riemannian manifold will always form a sequence of positive numbers $\lambda_1 \leq \lambda_2 \leq \lambda_3 \leq \cdots \to +\infty$ where each eigenvalue can be repeated only finitely many times. This set of eigenvalues is called the Laplace spectrum of the manifold. When a spectral geometer asks "can you hear the shape of a manifold" they are really asking "given the Laplace spectrum of a Riemannian manifold, what can be said about the geometry or topology of the manifold?"

We have seen that the Laplace spectrum of a string determines the shape of the string as we can determine its length from the lowest eigenvalue. This might lead us to believe that the Laplace spectrum of a manifold determines the shape of the manifold. However this is not the case: it is possible for two differently shaped manifolds to have identical Laplace spectra or, more informally, "sound the same." The first example of a pair of manifolds with this property was given by John Milnor in 1964 in a one page paper (!!) in the Proceedings of the National Academy of Science [29, 21]. Milnor constructed isospectral (having the same Laplace spectrum), non-isometric (having different shapes) 16-dimensional tori. This remarkable example weaves together number theory (modular forms), algebra (Leech lattices),

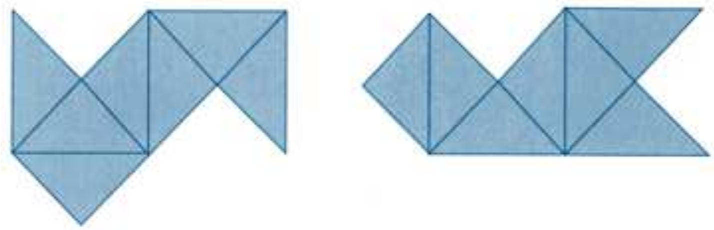

Figure 1.4. Laplace isospectral non-isometric planar domains

and analysis (the Poisson summation formula).

With Milnor's foundational result established, the floodgates were opened to questions in spectral geometry. Which features of a manifold are determined by its Laplace spectrum? Which features are not? How many different manifolds can share the same Laplace spectrum? Can a manifold be deformed in a way that leaves its Laplace spectrum unchanged? Many results have been obtained over the last five decades and many questions are still being investigated. The shapes in Figure 1.4 were discovered in 1992 by Carolyn Gordon, David Webb and Scott Wolpert [19] and are the most famous example of "drums that sound the same." These planar domains are non-congruent but share exactly the same Laplace spectrum. Interestingly, it can be shown that the Laplace spectrum does determine the area and the perimeter of a planar domain. By counting triangles, or edges of triangles, in Figure 1.4 you can check that this is indeed true for these two shapes.

1.3.2 From drums to imaging

Twenty years after Sir Arthur Schuster asked if one could detect the shape of a bell from the sound of its ringing, Russian mathematician Vladimir Steklov introduced a problem in 1902 [28] that has recently [17] caught the interest of spectral geometers. An applied interpretation of the problem is to seek a non-destructive way to detect cracks in the interior of a bridge support. The imaging method called "electrical impedance tomography [EIT]" provides a way to scan the interior of the support from its exterior [26]. In EIT electrodes are placed in a circle around a cross-section of the bridge support. A known amount of electrical current is then fed into the column. This current on the surface of the column induces an electrical potential field that crosses through its interior. The magnitude of this induced field is then measured by the ring of electrodes. In short: a current is input around the cross-section, it travels through the column, and the resulting output current around the cross-section is recorded. Because cracks on the interior of the column effect its conductivity, the way the input current transforms as it passes through the column can be used to construct a scan of the cross-section of the column. An example is given in Figure 1.5.

Viewing EIT from a more abstract perspective, we have a mapping between functions defined on the boundary of a cross-section of the column. The input current is transformed into the output current. The Steklov problem examines

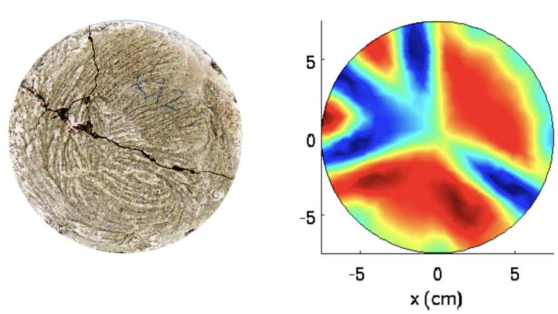

Figure 1.5. An EIT scan of a concrete column [36].

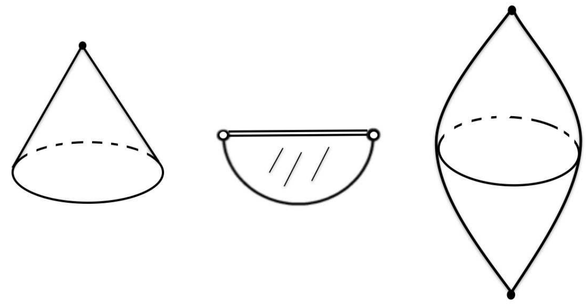

Figure 1.6. Three orbifolds: a cone, a folded disk, and a football.

this process in the mathematical setting of manifolds *with boundary*. The hemisphere in Figure 1.3 is an example of a manifold with boundary. If you trace the surface of the sphere or torus in Figure 1.3 with your finger, you will forever loop around and around the surface. However if you trace along the surface of the hemisphere you eventually arrive at the circular edge at the top of the hemisphere and have to stop. This circular edge is called the boundary of the hemisphere. Both the sphere and the torus have no boundary. Given a manifold M with boundary ∂M, the Steklov problem takes a function f defined on ∂M, extends it to a unique function $\tilde{f}$ on all of M for which $\Delta \tilde{f} = 0$, and returns a function $\mathcal{D}f$ defined on ∂M that records how quickly $\tilde{f}$ is changing near ∂M. (More precisely $\mathcal{D}f$ is the *normal derivative* of $\tilde{f}$ on ∂M.) The fact that $\Delta \tilde{f} = 0$, the Laplacian of $\tilde{f}$ is zero, means that $\tilde{f}$ is harmonic. Harmonic functions are used model the distribution of electrical charge over a region and provide the connection between the Steklov problem and its application to EIT. The operator $\mathcal{D}$, mapping f to $\mathcal{D}f$, is called the Dirichlet-to-Neumann operator.

The question from classical spectral geometry of determining the shape of a manifold from its Laplace spectrum neatly carries over to the Steklov setting. We derive information about the shape of a manifold with boundary from the infinite list of eigenvalues of the Dirichlet-to-Neumann operator on the boundary of the manifold. This list of eigenvalues is called the Steklov spectrum of the manifold and is written $0 \leq \sigma_1 \leq \sigma_2 \leq \sigma_3 \leq \cdots \to +\infty$. Examples of Steklov isospectral manifolds of dimension three [17] show that the Steklov spectrum of a manifold does not determine the shape of a manifold. However, in contrast to the Laplace spectrum setting, it is still not known if the Steklov spectrum determines the shape of a planar domain.

1.3.3 Contributions to spectral geometry

My work in spectral geometry studies the spectral properties of objects called Riemannian orbifolds. An orbifold is a generalized manifold arrived at by loosening the requirement that the space be locally modeled on R^n, and instead requiring it to be locally modeled on R^n modulo the action of a finite group. A Riemannian orbifold is obtained by requiring the space to be locally modeled on a Riemannian manifold modulo the action of a finite group of isometries. Although first defined by Satake over sixty years ago [**??**], the prevalence of these singular spaces in mathematics and physics (see [1, 3] for example), has generated interest in the properties of orbifolds.

Figure 1.6 shows three examples of two-dimensional orbifolds. On the left is a cone orbifold, shaped like a child's party hat. It is obtained as the quotient space when Z/nZ acts on the disk by rotations. In the middle is a half-disk orbifold which is the quotient of the disk under a reflection across a diameter. On the right is an orbifold called a 'football' that is a topological sphere with two cone points. To obtain the Z_n-football let Z_n act on a 2-sphere by rotations about an axis passing through the center of the sphere and take the quotient. The isotropy type of a point in an orbifold is the isomorphism class of the isotropy group of a lift of that point under the local group action. For example, the isotropy type of the cone points in the cone and football is Z/nZ. The isotropy type of the points on the upper edge of the half disk is $Z/2Z$. Those points in an orbifold with non-trivial isotropy are called singular points. Note that singular points in an orbifold can be isolated, as in the cone and the football, or appear in continua as in the half-disk.

A point in an orbifold is a boundary point if it is locally modeled on a half space $R^n_+ = \{(x_1, x_2, \dots, x_n) : x_n \geq 0\}$ modulo the action of a finite group. The boundary of the cone is the circle at its base. The boundary of the half-disk is the circular arc of points along its bottom edge, along with the two points indicated by circles on the top edge. This

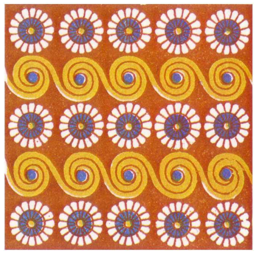

Figure 1.7. Pattern from an Egyptian tomb [25]

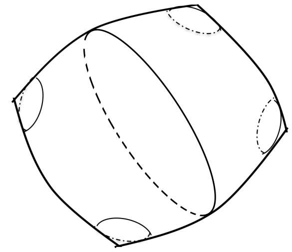

Figure 1.8. Pillow shaped 2-orbifold

boundary is itself a 1-dimensional orbifold obtained by taking the quotient of a circle by a reflection across a diameter. Note that the points in the half-disk drawn with a double line are singular points but not boundary points. The two points indicated by the open circles are both singular points and boundary points. The football has no boundary, just like the sphere and torus in Figure 1.3.

As a further source of examples, let us consider the beautiful class of 2-orbifolds associated wallpaper patterns. The quotient of the Euclidean plane under the symmetry group of a wallpaper pattern is either a smooth surface or a two-dimensional orbifold. The pattern in Figure 1.3.3 has translational and rotational symmetry. The corresponding quotient object is the four-cornered pillow orbifold shown in Figure 1.3.3. The four-cornered pillow has no boundary and has four singular points each with $Z/2Z$ rotational isotropy. To confirm this one can identify a fundamental domain for the symmetries of the wallpaper pattern, mark the edges of the fundamental domain with the appropriate glueings, and fold the fundamental domain into the pillow shape. H. Burgiel, J. Conway and C. Goodman-Strauss provide a similar treatment of all 17 wallpaper groups, and much more, in [10].

Can you hear the shape of an orbifold?

The focus of my dissertation work was the Laplace spectral geometry of Riemannian orbifolds. I examined the degree to which the Laplace spectrum of an orbifold determines the shape of the orbifold. Adapting existing comparison geometry techniques [7, 20, 4], I showed that any set of Laplace isospectral orbifolds, sharing a uniform lower sectional curvature bound, can contain orbifolds with only finitely many types BREAK OUT ISOTROPY TYPES HERE of singular points. In the special case of orbifolds with only isolated singularites, I also proved a universal upper bound on the number of singular points that may appear in any orbifold in the collection. The resulting paper [38] was the first publication to derive information about the singular points of an orbifold from the orbifold's Laplace spectrum.

My second paper [35] , joint with Naveed Shams and David Webb, was a response to the preceding one. We proved that the controls obtained in the preceding paper are the best possible. This was done by constructing large finite families of 26-dimensional orbifolds that all have the same Laplace spectrum, yet each possesses a distinct singular structure. SPECIFY THE FAMILIES AND QUOTE BUSER'S SUNADA (USED BY WEBB IN DRUMS ABOVE) These examples also showed that the Laplace spectrum doesn't determine the topology of the set of singular points in an orbifold.

In [33] Emily Proctor (one of my mathematical sisters) and I further developed the results of my disseration in the two-dimensional setting. We showed that in the presence of lower sectional curvature and volume bounds, as well as an upper diameter bound, techniques from comparison geometry can be used to bound the number of connected components of the singular set of a 2-orbifold. INCLUDE IMAGE OF GENERAL 2-OFD ORBISURFACE Using results from Farsi [14] we then showed that any collection of Laplace isospectral 2-orbifolds sharing a uniform lower sectional curvature bound contains only finitely many orbifold diffeomorphism types. This is the dimension two orbifold case of the n-manifold version of this statement obtained by B. Brooks, P. Perry and P. Petersen [7]. Proctor [31] extended our dimension two result to obtain orbifold homeomorphism finiteness of Laplace isospectral sets of n-dimensional orbifolds with only isolated singularties. John Harvey [22] later removed the requirement of only isolated singularities, fully extending the manifold homeomorphism finiteness result to the orbifold setting.

Proctor and I [32] also showed that, like manifolds, orbifolds can be continuously deformed in a way that preserves the Laplace spectrum. We constructed an isospectral deformation of metrics on an orbifold quotient of an infranilmanifold. The major tool used was a generalization of Sunada's Theorem due to DeTurck and Gordon [12].

I doubled my mathematical toolbox working with my postdoc mentor Alejandro Uribe. Our joint paper [] applies ideas from mathematical physics to understand the spectral properties of Riemannian orbifolds. The wave kernel $W(t,x,y)$ of a Riemannian manifold M is the integral kernel of the wave operator on M and has trace

$$\int_M W(t,x,x)\,\mathrm{dVol}(x) = \sum_j e^{-it\sqrt{\lambda_j}}$$

where λ_j denotes the jth Laplace eigenvalue of M. The wave trace is a distribution with singularities contained in the manifold's *geodesic length spectrum*, i.e. the list of lengths of closed geodesics in the manifold. The wave trace lets us conclude that the Laplace spectrum of a manifold (generically) determines its geodesic length spectrum and provides spectral invariants known as the *wave invariants* [13]. The motivation of my work with Uribe in [**?**] was to extend wave trace methods to the orbifold setting. Applying more general results by Kordyukov [27] and Sandoval [34] in the setting of Riemannian foliations, we provided an orbifold category construction of the wave trace and its asymptotic expansion for first-order symmetric elliptic pseudodifferential operators P with positive principal symbol (such as $\sqrt{\Delta}$). Although the wave trace results for orbifolds mirror those for manifolds, along the way we discovered an interesting orbifold-category feature of the *spectral function* of an orbifold. Let $\{\psi_j\}$ denote an orthonormal basis of eigenfunctions of the operator $\sqrt{\Delta}$ (or more generally P as above) on orbifold X. Fixing $x_0 \in X$, we found that the the asymptotic behavior as $t \to \infty$ of the spectral function

$$\mathcal{S}(t) = \sum_{\sqrt{\lambda_j} \le t} |\psi_j(x_0)|^2$$

on X depended on the isotropy type of the point x_0. In particular we found that eigenfunctions ψ_j have, on average, larger magnitude at singular points than at manifold points by a factor of the order of the isotropy group.

MENTION LEARING ABOUT PSIDOS TO TRANSISTION TO STEKLOV WORK

The Steklov spectrum of an orbifold

SOME DETAIL ON INVERSE TOMOGRAPHY QUESTION AND IMAGE - BORROW DISK STUFF FROM TALK STATE MANIFOLD SETTING RESULT (SURFACES)
Here I summarize the results of the paper *Spectral Geometry of the Steklov problem on orbifolds* by T. Arias-Marco, E. Dryden, C. Gordon, A. Hassannezhad, A. Ray, and myself, accepted by International Mathematics Research Notices, [2]. (Because this is a mathematics paper, the conventions of the mathematics community are followed and authors are listed in alphabetical order.)

Note that results (c) and (d) suggest that the study of the Steklov spectrum on orbifolds is of interest not only because orbifolds are themselves interesting, but also because this study can shed light on questions in the manifold setting.

(a) We showed that the Steklov spectrum of a two-dimensional orbifold with boundary determines the number of singular points on the boundary of the orbfiold. In fact, generalizing work of [16] from the smooth setting, we showed that the Steklov spectrum of a two-dimensional orbifold with boundary determines the boundary of the orbifold up to an equivalence relation.

(b) In dimension two, we used facts about the shape of an orbifold to compute bounds on the size of each number in the Steklov spectrum. More precisely, we found eigenvalue bounds in terms of the orbifold's Euler characteristic and the topology of the boundary of the orbifold.

(c) We extended results of [9, 23] to obtain upper bounds on the Steklov eigenvalues of an n-dimensional orbifold in terms of the isoperimetric ratio and a conformal invariant, gaining a sharpness result on these bounds that was not available in the manifold setting.

(d) We gave examples of different (non-isometric) orbifolds with the same Steklov spectrum that possess various properties. We also provide a two-dimensional counterexample to the inverse tomography problem in the orbifold setting. The inverse tomography problem takes as given not just the Steklov spectrum of an orbifold, but the entire Dirichlet-to-Neumann operator. Although surfaces without singular points are determined uniquely by their Dirichlet-to-Neumann operator, this is not true in the orbifold setting. The counterexample we provide is very simple: we show that the standard disk of radius k (k a natural number) and a flat cone with cone angle $\frac{2\pi}{k}$ have the same Dirichlet-to-Neumann operator.

LOCATING THIS WORK IN MY RESEARCH TRAJECTORY

1.4 Discipline-based pedagogical research

From the Fall of 2012 until the Summer of 2017 I served as associate director, then director, of the program funded by Lewis & Clark College's institutional Howard Hughes Medical Institute (HHMI) grant. As one of my first activities for the program I attended a meeting hosted by HHMI for grant directors at undergraduate institutions. At this meeting I learned about the national level problem posed to undergraduate life sciences education by students with insufficient mathematical preparation. Despite calls to strengthen the quantitative preparation of life science students [11, 39, 30, 15], little evidence had been collected to identify interventions that were successful in improving the quantitative performance of these students. I was intrigued by this problem and discussed it with many conference attendees. The four-day meeting closed with a surprise opportunity to apply for collaborative subgrant-funded projects related to our main grant programs. A six-member grant writing team formed around the idea of assessing life science student preparation in quantitative topics. Within a month we had secured funding and I became a 'DBER,' that is a Discipline-Based – holding a Ph.D. in STEM, not in education – Education Researcher.

The team expanded to include myself, undergraduate chemistry and biology faculty, educational psychologists, and a college institutional research staff member.[3] We developed a multiple choice assessment called the $BioSQuaRE$ to measure student proficiency with sophomore-level quantitative biology. Our paper [37] describes the development of the assessment and serves as a roadmap for other discipline-based education researchers interested in developing robust assessments of courses or programs.

In the test development process a test is written under the hypothesis that scores on the test measure a specific latent trait of a student. We defined the latent trait of a student that we hoped to measure by reading biology education literature and consulting with biology faculty. Through this we built an understanding of what quantitative skills biology students should possess after they have completed a colleg-level introductory biology sequence. This set of skills, which we called "quantitative reasoning in a biological context," was the latent trait of a student that we sought to measure. Guided by literature in test development, we transformed our understanding of quantitative reasoning in a biological context into a test blueprint for the $BioSQuaRE$, wrote or adapted questions to match the test blueprint, and then piloted and edited the $BioSQuaRE$ in six iterative cycles.

After the piloting process, psychometric analysis was performed on data from a sample of 555 students who took the most refined version of the $BioSQuaRE$. Internal consistency measured by coefficient alpha met the accepted threshold to be deemed 'very good.' Tests of the model-level and item-level fit of the Rasch model (a psychometric statistical model for analyzing categorical data) to our data set were performed, and it was determined that the data was a reasonable fit to the Rasch model. The Rasch model indicated that the $BioSQuaRE$ tests the visualization of quantitative ideas in the context of biology at a range of student ability levels. Also the $BioSQuaRE$ tests statistical concepts particularly well among students of lower ability, and tests algebraic concept particularly well among students of higher ability. Overall the $BioSQuaRE$ contains items that test abilities in a range two standard deviations above and below average ability. This analysis also indicated that the $BioSQuaRE$ was particularly good at discriminating between the ability levels

Because most refined version of the $BioSQuaRE$ has strong enough test properties to use in assessing quantitative reasoning in a biological context, we have implemented it online for educators to use freely. It is the hope of the Biosquare team that the assessment will help educators to identify what works best in preparing biology students with quantitative skills. Since 2016, the BioSQuaRE has been used by twelve institutions outside of the original consortium, coming from five different categories in the Carnegie Classification. As students complete the exam, results are pooled

[3] The full team is: myself, Laura Ziegler (Iowa State University), Tabassum Haque (Oberlin College), Laura Le (University of Minnesota), Marcelo Vinces (Oberlin College), Gregory K. Davis (Bryn Mawr College), Andy Zieffler (University of Minnesota), Peter Brodfuehrer (Bryn Mawr College), Marion Preest (Keck Science Department of Claremont McKenna, Pitzer and Scripps Colleges), Jason Belisky (Oberlin College), Charles Umbanhowar, Jr. (St. Olaf College), and Paul J. Overvoorde (Macalester College).

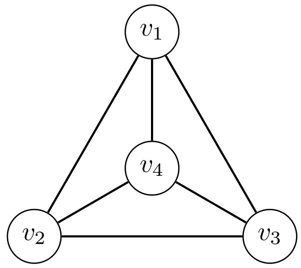

Figure 1.9. A graph with four vertices and six edges

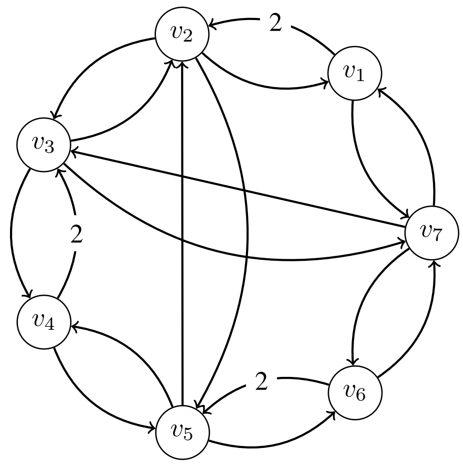

Figure 1.10. a 3-orbigraph with 7 vertices

to gain a national perspective on the quantitative skills of biology students. We expect as more institutions use the BioSQuaRE the national baseline of scores formed will become increasingly useful. One institution reports that use of the BioSQuaRE in pre/post assessment of its introductory biology sequence has increased understanding of the skill level of entering students as well as growth in student probability and statistics skills. Also, the BioSQuaRE was part of the assessment plan used in a recent study of implicit instruction of quantitative and statistics skills in biology (Beck, 2018).

1.5 Undergraduate research into orbifold graphs

In the mathematical field of graph theory, the word *graph* refers to a network of *vertices* (also called *nodes*) connected by lines called edges. Figure 1.9 gives an example of a graph with four vertices and six edges. A basic tool in graph theory is the *adjacency matrix* of a graph. The adjacency matrix is a grid of numbers where a 1 in jth column of the ith row means that there is an edge in the graph connecting vertex v_i to vertex v_j. A 0 in the same location of the adjacency matrix indicates that there is no edge between vertex v_i and vertex v_j. The adjacency matrix of the graph in Figure 1.9 is

$$\begin{bmatrix} 0 & 1 & 1 & 1 \\ 1 & 0 & 1 & 1 \\ 1 & 1 & 0 & 1 \\ 1 & 1 & 1 & 0 \end{bmatrix}.$$

In spectral geometry a manifold or an orbifold is studied using its Laplace spectrum or its Steklov spectrum. In spectral graph theory a graph is studied using its graph spectrum. The spectrum of a graph is a finite list of numbers associated to the graph. There are several different ways to define the spectrum of a graph. A straightforward approach is to use the adjacency matrix of the graph. In particular, I define the spectrum of a graph to be the eigenvalue spectrum of the adjacency matrix of the graph. For example, the spectrum of the graph in Figure 1.9 is $3, -1, -1, -1$ because these numbers are the eigenvalues of the graph's adjacency matrix (given above).

There are interesting connections between the study of the spectral properties of a manifold and the study of the spectral properties of a graph. For example, one can ask if the Laplace spectum of a manifold determines the volume of the manifold. The analogous question in spectral graph theory is to ask if the spectrum of a graph determines the number of vertices in the graph. (The answer to both questions is yes.) The strong relationship between spectral graph theory and spectral geometry has been a subject of great interest to mathematicians (for example see [8, 40, 6]).

As a spectral geometer who works with undergraduates I find graph theory to be a good source of undergraduate research problems. Graphs are easier to work with than manifolds or orbifolds, and the questions of spectral graph theory are familiar to me from my work in spectral geometry. Because my contributions to spectral geometry focus on the properties of orbifolds, my motivating question in spectral graph theory is "Can we define a graph theoretic analogue of an orbifold that has interesting spectral properties?"

SUMMARY OF RESULTS OBTAINED ABOUT THE SPECTRAL PROPERTIES OF ORBIGRAPHS

Here I summarize the results of the manuscript *Orbigraphs: A Graph Theoretic Analog to Riemannian Orbifolds* by K. Daly, C. Gavin, G. Montes de Oca, D. Ochoa, myself, and S. Stewart. Although this paper is in final form, I plan to submit this paper for publication in July 2017 in order to give each co-author sufficient time for a final read through. (Because this is a mathematics paper, the conventions of the mathematics community are followed and authors are listed in alphabetical order.)

In this manuscript we defined a graph theoretic analogue of an orbifold called an *orbigraph* and showed several topological and spectral properties of orbigraphs. Our formulation of the definition of an orbigraph was based on [6] where Brooks described an "orbifold graph" as the quotient of a regular graph under a non-free group action. However Brooks didn't develop the idea further. Our definition adapted the process of taking the quotient of a k-regular graph under an equitable partition, a global process, to a local process of taking the quotient of a k-star by an equitable partition. The quotient k-stars are then assembled to form directed graphs and these directed graphs are orbigraphs. In this way we mirror the definition of an orbifold as an object that is locally the quotient of a manifold under the action of a finite group of homeomorphisms.

The topological properties of orbigraphs that we determined are the following.

(a.) Some vertices in an orbigraph have the same local structure as a vertex in a k-regular graph and some do not. This allowed us to define regular and singular vertices in an orbigraph.

(b.) We showed that some orbigraphs can be obtained as the quotient of a finite k-regular graph under an equitable partition and some cannot. This mirrors the covering properties of good versus bad orbifolds.

(c.) We used the theory of Markov chains to characterize precisely when an orbigraph can be obtained as the quotient of a finite k-regular graph.

When we studied the spectral properties of orbigraphs, we focused on spectral results that are specific to the setting of orbigraphs. We showed the following.

(a.) We provided an example that shows that the spectrum does not detect whether or not an orbigraph can be obtained as the quotient of a finite k-regular graph.

(b.) We showed that the number of singular points in an orbigraph can be bounded both above and below by spectrally-determined quantities.

(c.) We showed that the spectrum of an orbigraph does detect the presence of singular points. That is, we showed that a regular graph and an orbigraph with one or more singular points cannot have the same spectrum. The analogous question in the setting of the Laplace spectrum of orbifolds is still open.

1.6 Future work

What are the major questions that have yet to be solved? What are you working on now (if you're comfortable sharing that)?

We are currently seeking to understand what orbifold surface maximizes the second number in the Steklov spectrum among orbifold surfaces with a specific perimeter (if such a maximizer exists). In particular we are curious about how Weinstock's inequality [41], and its generalizations, extend to the setting of two-dimensional orbifolds.

A second phase of the $BioSQuaRE$ project is currently underway. We are following a cohort of incoming biology students in order to track how well $BioSQuaRE$ scores correlate with entrance exam (SAT, ACT) scores as well as with performance in biology courses. This second project will provide further evidence that the $BioSQuaRE$ is a useful instrument to measure quantitative skills in the context of biology. It is likely this second project will result in another publication. In July 2017 the $BioSQuaRE$ team will regroup to analyze the first year's worth of data from this longitudinal study, as well as to determine the next steps for the project.

1.7 Bibliography

[1] Alejandro Adem, Jack Morava, and Yongbin Ruan (eds.), *Orbifolds in mathematics and physics*, Contemporary Mathematics, vol. 310, Providence, RI, American Mathematical Society, 2002. MR 2003g:00020

[2] T. Arias-Marco, E. Dryden, C. S. Gordon, A. Hassannezhad, A. Ray, and E. Stanhope, *Spectral geometry of the steklov problem on orbifolds*, Int. Math. Res. Not. (2017).

[3] Michel Boileau, Bernhard Leeb, and Joan Porti, *Geometrization of 3-dimensional orbifolds*, Ann. of Math. (2) **162** (2005), no. 1, 195–290. MR 2178962

[4] Joseph E. Borzellino, *Orbifolds of maximal diameter*, Indiana Univ. Math. J. **42** (1993), no. 1, 37–53. MR 94d:53053

[5] William E. Boyce and Richard C. DiPrima, *Elementary differential equations and boundary value problems*, John Wiley & Sons, Inc., New York-London-Sydney, 1965. MR 0179403

[6] Robert Brooks, *Non-Sunada graphs*, Ann. Inst. Fourier (Grenoble) **49** (1999), no. 2, 707–725. MR 1697378 (2000i:58062)

[7] Robert Brooks, Peter Perry, and Peter Petersen, V, *Compactness and finiteness theorems for isospectral manifolds*, J. Reine Angew. Math. **426** (1992), 67–89. MR 93f:53034

[8] Fan R. K. Chung, *Spectral graph theory*, CBMS Regional Conference Series in Mathematics, vol. 92, Published for the Conference Board of the Mathematical Sciences, Washington, DC; by the American Mathematical Society, Providence, RI, 1997. MR 1421568

[9] B. Colbois, A. El Soufi, and A. Girouard, *Isoperimetric control of the Steklov spectrum*, J. Funct. Anal. **261** (2011), no. 5, 1384–1399. MR 2807105

[10] John H. Conway, Heidi Burgiel, and Chaim Goodman-Strauss, *The symmetries of things*, A K Peters, Ltd., Wellesley, MA, 2008. MR 2410150

[11] National Research Council, *Bio2010: Transforming undergraduate education for future research biologists*, The National Academies Press (2003).

[12] Dennis M. DeTurck and Carolyn S. Gordon, *Isospectral deformations. II. Trace formulas, metrics, and potentials*, Comm. Pure Appl. Math. **42** (1989), no. 8, 1067–1095, With an appendix by Kyung Bai Lee. MR 1029118 (91e:58197)

[13] J. J. Duistermaat and V. W. Guillemin, *The spectrum of positive elliptic operators and periodic bicharacteristics*, Invent. Math. **29** (1975), no. 1, 39–79. MR MR0405514 (53 #9307)

[14] Carla Farsi, *Orbifold spectral theory*, Rocky Mountain J. Math. **31** (2001), no. 1, 215–235. MR 2001k:58060

[15] American Association for the Advancement of Science, *Vision and change in undergraduate biology education: A call to action*, AAAS (2011).

[16] A. Girouard, L. Parnovski, I. Polterovich, and D. Sher, *The Steklov spectrum of surfaces: asymptotics and invariants*, Math. Proc. Cambridge Philos. Soc. **157** (2014), no. 3, 379–389. MR 3286514

[17] Alexandre Girouard and Iosif Polterovich, *Spectral geometry of the Steklov problem (survey article)*, J. Spectr. Theory **7** (2017), no. 2, 321–359. MR 3662010

[18] C. Gordon and D. Webb, *You Can't Hear the Shape of a Drum*, American Scientist **84** (1996), 46–55.

[19] C. Gordon, D. Webb, and S. Wolpert, *Isospectral plane domains and surfaces via Riemannian orbifolds*, Invent. Math. **110** (1992), no. 1, 1–22. MR 1181812

[20] Karsten Grove and Peter Petersen, V, *Bounding homotopy types by geometry*, Ann. of Math. (2) **128** (1988), no. 1, 195–206. MR 90a:53044

[21] J. Harthong and H. Rubenthaler, *Contre exemple de Milnor*, (1973), 30. MR 0650999

[22] John Harvey, *Equivariant Alexandrov geometry and orbifold finiteness*, J. Geom. Anal. **26** (2016), no. 3, 1925–1945. MR 3511464

[23] A. Hassannezhad, *Conformal upper bounds for the eigenvalues of the Laplacian and Steklov problem*, J. Funct. Anal. **261** (2011), no. 12, 3419–3436. MR 2838029

[24] Pierre Janssen and Norman Lockyer, C. R. Acad. Sci. Paris **67** (1868), 836841.

[25] O. Jones, *The grammar of ornament*, Quaritch, 1910, `http://digital.library.wisc.edu/1711.dl/DLDecArts.GramOrnJones`.

[26] Kimmo Karhunen, Aku Seppänen, and Jari P. Kaipio, *Adaptive meshing approach to identification of cracks with electrical impedance tomography*, Inverse Probl. Imaging **8** (2014), no. 1, 127–148. MR 3180415

[27] Yu. A. Kordyukov, *The trace formula for transversally elliptic operators on Riemannian foliations*, Algebra i Analiz **12** (2000), no. 3, 81–105. MR MR1778191 (2001h:58037)

[28] Nikolay Kuznetsov, Tadeusz Kulczycki, Mateusz Kwaśnicki, Alexander Nazarov, Sergey Poborchi, Iosif Polterovich, and Bartł omiej Siudeja, *The legacy of Vladimir Andreevich Steklov*, Notices Amer. Math. Soc. **61** (2014), no. 1, 9–22. MR 3137253

[29] J. Milnor, *Eigenvalues of the Laplace operator on certain manifolds*, Proc. Nat. Acad. Sci. U.S.A. **51** (1964), 542. MR 0162204

[30] Association of American Medical Colleges-Howard Hughes Medical Institute Joint Committee, *Scientific foundations for future physicians*, AAMC (2009).

[31] Emily Proctor, *Orbifold homeomorphism finiteness based on geometric constraints*, Ann. Global Anal. Geom. **41** (2012), no. 1, 47–59. MR 2860396

[32] Emily Proctor and Elizabeth Stanhope, *An isospectral deformation on an infranil-orbifold*, Canad. Math. Bull. **53** (2010), no. 4, 684–689. MR 2761691

[33] ———, *Spectral and geometric bounds on 2-orbifold diffeomorphism type*, Differential Geom. Appl. **28** (2010), no. 1, 12–18. MR 2579379

[34] Mary R. Sandoval, *Wave invariants of the spectrum of the G-invariant Laplacian and the basic spectrum of a Riemannian foliation*, Comm. Partial Differential Equations **33** (2008), no. 10-12, 1818–1846. MR MR2475320 (2009m:58067)

[35] Naveed Shams, Elizabeth Stanhope, and David L. Webb, *One cannot hear orbifold isotropy type*, Arch. Math. (Basel) **87** (2006), no. 4, 375–384. MR 2263484

[36] S. Siltanen, *Accessed may 29 2018*, 2016, `http://www.siltanen-research.net/IPexamples/eit/eit_and_its_applications`.

[37] E. Stanhope, L. Ziegler, T. Haque, L. Le, M. Vinces, G. Davis, A. Zieffler, P. Brodfuehrer, M. Preest, J. Belisky, C. Umbanhowar Jr., and P. Overvoorde, *Development of a biological science quantitative reasoning exam (BioSQuaRE)*, CBE Life Sciences Education, to appear.

[38] Elizabeth Stanhope, *Spectral bounds on orbifold isotropy*, Ann. Global Anal. Geom. **27** (2005), no. 4, 355–375. MR MR2155380 (2006g:58059)

[39] Next Generation Science Standards Lead States, *Next generation science standards: For states, by states*, The National Academies Press (2013).

[40] Toshikazu Sunada, *Riemannian coverings and isospectral manifolds*, Ann. of Math. (2) **121** (1985), no. 1, 169–186. MR 86h:58141

[41] Robert Weinstock, *Inequalities for a classical eigenvalue problem*, J. Rational Mech. Anal. **3** (1954), 745–753. MR 0064989

[42] XKCD, *accessed may 22 2018*, 2016, `https://xkcd.com/1733/`.